THE EFFECT OF BUOYANCY ON OPPOSED SMOLDERING

A. Bar-Ilan, G. Rein, D.C. Walther, A.C. Fernandez-Pello[1]

Department of Mechanical Engineering
University of California
Berkeley, CA 94720, USA

J.L. Torero

School of Engineering and Electronics
University of Edinburgh, Edinburgh EH9 3JN, UK

D.L. Urban

NASA Glenn Research Center
Cleveland, OH 44135, USA

Published in:

Combustion Science and Technology, Vol. 176, 2004, pp. 2027-2055.

[1] Corresponding author; ferpello@me.berkeley.edu

ABSTRACT

An experimental investigation on the effects of buoyancy on opposed flow smolder is presented. Tests were conducted on cylindrical samples of open-cell, unretarded polyurethane foams at a range of ambient pressures using the Microgravity Smoldering Combustion (MSC) experimental apparatus. The samples were tested in the opposed configuration, in which the flow of oxidizer is induced in the opposite direction as the propagation of the smolder front. These data were compared with opposed forced-flow tests conducted aboard STS-69, STS-77, and STS-105 and their ground based simulations. Thermal measurements were made of the smolder reaction to obtain peak reaction temperatures and smolder velocities as a function of the ambient pressure in the MSC chamber. The smolder reaction was also observed using high-frequency ultrasound pulses as part of the Ultrasound Imaging System (UIS). The UIS measurements were used as a second means of providing smolder propagation velocities as well as to obtain permeabilities of the reacting samples. Results of forced flow testing in normal gravity were compared to results in microgravity at a range of ambient pressures and forced flows. Results indicate that a critical oxidizer mass flux of roughly 0.5 to 0.8 g/m^2s is required in normal gravity for a self-sustaining propagation in this configuration. In microgravity tests, self-sustained smolder propagation was observed at a significantly lower oxidizer mass flux of 0.30 g/m^2s. Analysis suggests that the removal of buoyancy-induced heat losses in microgravity allows for self-sustained propagation at an oxidizer mass flux below the critical value observed in normal-gravity testing. Normal-gravity tests also show that the smolder propagation velocity is linearly dependent on the total oxidizer mass flux in an oxidizer-limited regime. Pressure effects on the chemical kinetics of a smolder reaction are inferred by comparison of normal-gravity and microgravity tests and believed to be only weakly dependent on pressure ($\sim P^{1/3}$).

Keywords: Smoldering Combustion; Microgravity; Opposed Flow; Buoyancy Effects; Heat Losses

I. INTRODUCTION

Propagation of in-depth smolder combustion presents an important fire risk because the smolder reaction spreads very slowly through the interior of porous fuels and thus can go undetected for a long time. Also the products of smolder are very toxic, although produced at smaller rates than in flaming fires. Smolder of cable insulation, cellulose and polymeric foam materials is of concern in fire-safety because of the prevalence of these materials in many aspects of industry as well as everyday life. Smolder-initiated fires account for 30% of residential fire deaths, both due to a sudden transition from smoldering to flaming and due to the higher rate of toxic species production (Hall 2003, Damant 1994, Babrauskas 1996). Smoldering is also of concern in NASA spacecraft and space installations – to date there have been a few minor incidents of overheated and charred cables and electrical components reported on Space Shuttle flights (Friedman 1993, Ross 1997) and significant smolder-related incidents aboard the Russian space station Mir (Burrough 2000). The establishment of the International Space Station, and the potential for future long duration manned space missions, has increased the interest in the study of smoldering in reduced gravity because of the need to preempt the possibility, and to minimize the effect of a smolder-initiated fire during the operation of these facilities. The effect of buoyancy on smolder is also relevant for this purpose because, due to the high cost of testing in space-based laboratories, most of the smolder combustion studies have to be conducted in normal gravity and the results applied to microgravity.

It is well established that smolder propagation is strongly dependent on the mass flux of oxidizer to the smolder front (Ohlemiller 1985, Dosanjh 1987). Gravity can induce complex buoyant flows through the porous material and as a result affect smolder propagation through a buoyantly induced oxidizer-mass flux (Torero, 1993, Torero et al. 1993). Consequently, it is of interest to study the effects of buoyancy on smolder not only to understand smoldering propagation in normal gravity but also to extend the results to microgravity environments.

For a fixed fuel permeability and sample length, the buoyant flow of oxidizer through the porous material interior can be varied by either changing the gravity acceleration or by varying the ambient pressure. Following this approach, a series of tests were conducted on forced flow opposed smolder through polyurethane foam in microgravity, and in normal gravity at varying ambient pressures. The experiments are used to determine the dependence of the smolder process on the forced- and buoyant-convection mass fluxes. Also, since the smolder chemical reaction potentially depends on the ambient pressure, an additional result of the work is the identification of the dependence on pressure of the smolder chemical kinetics during self-sustained propagation. Furthermore, determination of the effects of pressure on the physical mechanisms governing smoldering combustion could also provide a better understanding of smolder in closed systems like bulkheads, submarines, and spacecraft in which elevated or reduced pressure environments may be encountered.

The microgravity experiments are conducted in the NASA Space Shuttle because of the need for long testing times. Space-based experiments are difficult to conduct because of their high cost, and consequently the number of tests is generally limited, making each test very valuable because of its uniqueness. In this work the results from a microgravity forced opposed-flow smolder test with polyurethane foam as fuel conducted during the Space Shuttle STS-108 mission (December 2001), are presented in detail first. These data have not been previously reported and provide new interesting information on the smolder process obtained with a newly implemented ultrasound probing system. The data from this test are used together with that from two other previously reported tests (Walther et al. 1999) conducted at different airflow velocities to determine the dependence of smolder on the oxidizer-mass flux to the smolder front. Normal-gravity

simulations of these tests together with complementary tests conducted varying elevated pressures are used to determine the effect of buoyancy on the smolder propagation.

II. EXPERIMENTAL HARDWARE AND PROTOCOL

The microgravity and normal gravity experiments were conducted in the flight hardware of the Microgravity Smolder Combustion (MSC) experiment, a project funded by NASA to study smolder combustion in micro-gravity. A schematic diagram of the experimental hardware is shown in Fig. 1 and described in detail in Walther et al. (1999). The test duct, located in a 21.7 liters, semi-cylindrical, hermetically sealed aluminum combustion chamber (Fig. 1), consists of a 120 mm diameter, 140 mm long, cylindrical sheath where a polyurethane foam sample is held, an igniter at one end of the sheath and a flow inlet at the other end. The sample holder sheath is 3 mm thick and was initially made of quartz (Space Shuttle missions STS-69 and STS-77), and later of Vespel (STS-105). The sheath change was needed to incorporate an Ultrasound Imaging System (UIS) described below. A cylindrical porous ceramic disc igniter is placed at one end of the sample holder sheath in contact with the fuel. The igniter consists of a length of Nichrome wire of known resistance wound in a four-lobe pattern on a sandwich of two honeycomb-celled Cordierite ceramic plates of 120 mm diameter. During ignition, the igniter in the first two tests (STS-69, 77) was activated with a ramped power to provide a predetermined temperature rise rate in the foam near the igniter, and the last test (STS-105) with a constant power for a predetermined period of time. The latter protocol was selected in order to provide a shorter duration of igniter activation so that self-smolder propagation at the higher oxidizer mass flux of the STS-105 experiment could be observed without the igniter influence. A cylindrical metal housing, 120 mm diameter by 52 mm long, filled with char from a previously smoldered sample, or alternatively with porous Fiberfrax ceramic fiber insulation, is placed at the other side of the igniter, to simulate the insulating conditions that the char provides during the propagation of the smolder reaction. A cap with the airflow inlet is fitted at the end of the fuel sample sheath opposite to the igniter, such that the air flows opposite to the direction of smolder propagation (opposed smolder). A predetermined and constant flow of air is forced through the foam sample via regulated pressure upstream of a choked flow orifice in the microgravity experiments and with a mass flow controller (MFC) in the normal gravity experiments. No recirculation effects have been observed because the controlled flow is provided from a source external to the chamber.

The fuel samples consist of cylinders, 132 mm diameter by 150 mm long, of open-cell, unretarded, polyurethane foam of 26.5 kg/m^3 density and 0.975 void fraction. The foam samples are inserted into the cylindrical sample sheath, providing a volumetric compression of approximately 10% to reduce the oxidizer flow between the walls of the sample and the sheath, a channeling effect observed in rigid porous materials (Nield and Bejan 1992). Polyurethane foam is selected as fuel because it is representative of materials commonly used on both earth and space based facilities, its material properties are well known, and it maintains its structural integrity upon smoldering.

The foam sample is instrumented with an array of ten type-k, sheathed thermocouples with a wire diameter of 0.08 mm, which provide axial and radial temperature histories of the foam and char during smolder. Two of the thermocouples are located on the igniter itself, and six others are inserted into the foam at the centerline spaced 20 mm apart in the axial direction. Two other thermocouples are placed radially at the center of the sample. The thermocouple locations are described in detail in Walther et al. (1999). For the tests of the STS-105 mission, and the normal gravity experiments following it, in addition to the thermocouples, a novel ultrasonic imaging system (UIS) developed for the MSC project (Tse et al. 1998) is applied to image the interior of the foam and determine the permeability of the material. The UIS allows for monitoring non-

intrusively the smolder reaction because the passage of a smolder front leaves behind a char of significantly higher permeability than the unburned foam (up to several orders of magnitude), and the attenuation of the ultrasound signal is proportional to the inverse square root of the permeability (Tse et al. 1998). For this purpose, the initially used quartz sample holder was replaced with one made of Vespel (polycarbonate) to increase the transmission of the ultrasound signal through the sheath. It has been found that the quartz sheath leads to reflection of the ultrasonic signal, which generates significant noise in the received signal. The sheath is perforated to accommodate a set of five ultrasonic speaker/microphone transducer pairs (Fig. 1) that are fixed lengthwise along the sheath to obtain line-of-sight average permeability data of the foam. The first speaker microphone pair is located 20 mm from the surface of the igniter, the second pair is 35 mm from the first and the remaining transducer pairs are spaced at 20 mm increments, which coincides with the location of the axial thermocouples. All speakers are driven simultaneously, emitting a 40 kHz wave train pulse consisting of 6 cycles, with a 150 V peak-to-peak amplitude after amplification. With this arrangement line-of-sight average permeability can be measured at specific locations corresponding to the positions of the speaker and microphone pairs. By monitoring changes in permeability with the UIS it is possible to image the location of the smolder reaction, and the level of fuel consumption by the reaction, and consequently determine the smolder velocity and strength of the reaction.

The thermocouples output is used to obtain velocity measurements of the smolder propagation front and reaction temperatures. The smolder propagation velocity is calculated through the time of arrival of the smolder front to successive thermocouples, and the separation between the thermocouples (Torero et al. 1993). Similar to the thermocouple histories, the UIS histories display sharp rates-of-rise in signal as the smolder propagation front passes a speaker/microphone pair, and a similar method to that used with the thermocouples is used to determine smolder propagation velocities. The results are used to verify the smolder propagation velocities determined from the thermocouples output.

For the microgravity experiments, the combustion chambers, compressed air and instrumentation assembly are integrated into a Get Away Special Canister (GAS-CAN), which is flown in the Space Shuttle cargo bay. A photograph of the assembly is shown in Fig. 2. Igniter power, pressure, temperature and ultrasound data are recorded during the smolder of each foam sample. Gases and remaining char samples from the tests are stored inside the chamber until removal post-flight. The normal gravity experiments are conducted in a single MSC sealed chamber with the corresponding instrumentation. It is important to note that because the chamber is sealed, the ambient pressure increases from 1 atm to up to 3 atm during the microgravity tests and the normal-gravity simulations, due to the addition of air and the increase in the chamber gas temperature. This can affect the smolder reaction rate from chemical kinetic pressure effects. In the normal gravity simulation tests there is also the added effect of the increase in the buoyant air flow through the sample, and of the heat losses to the surrounding environment as the pressure increases.

To further study the effect of buoyancy on smolder, another series of normal gravity tests were conducted at a constant ambient pressure, in the range from 1 atm to 3 atm. As with the other normal gravity experiments, the tests are conducted in a single MSC chamber but with a pressure regulator to maintain the chamber at a prescribed constant pressure. Thus the tests reported here were conducted in opposed forced flow in microgravity, and opposed forced flow in normal gravity with an increasing pressure for the simulation tests, and a constant pressure for the pressure tests. A schematic of this configuration is shown in Figure 3.

The microgravity and normal gravity experiments were conducted with forced air mass fluxes of 0 (quiescent), 1.22, 2.44 and 3.66 g/m^{2}s. The results from the 3.66 g/m^{2}s (STS 105 mission), which includes the UIS data, are described in detail here since they are new. As mentioned above the sample sheath of this experiment was made of Vespel, which has a lower thermal and electrical conductivity than quartz. Also the igniter was powered with 90 W for 600 s rather than 70 W for 1200 s as used in the previous two tests to reduce the time of influence of the igniter on the smolder process. The normal gravity forced flow experiments were conducted with a setup and igniter setting similar to those of the forced flow microgravity tests, and with the test section placed vertical. The simulations were conducted both with the igniter at the top and the air inlet at the bottom, so that the smolder reaction progressed downward with the forced flow assisted by buoyancy, and with the test section rotated 180° so that the smolder reaction progressed upward with the downward forced flow deterred by buoyancy. As in the microgravity tests, the chamber in the simulation tests was sealed and the pressure increased as the test progressed. Another series of normal gravity tests were conducted in the downward configuration, and at a constant predetermined chamber pressure that was regulated to within ±1 psi (0.068 atm) during the experiments, so that the buoyant mass flux could be varied.

III. EXPERIMENTAL RESULTS

The primary results of the smolder tests conducted here are the smolder propagation velocity, smolder reaction temperature, and char permeability. The characteristics of the smolder ignition are obtained from the igniter power data, and the temperature histories provided by the thermocouples on the igniter and in the foam near the igniter. The data from the thermocouples placed along the foam sample centerline are used for calculating the propagation velocity of the smolder reaction, as well as the intensity of the smolder reaction. The line-of-sight average permeability histories provide char permeability (fuel completion) data as well as a second non-intrusive measurement of the smolder propagation velocity.

III.1 Microgravity Experiments and Normal Gravity Simulations

The results of the microgravity experiments for the 3.66 g/m^{2}s forced air mass-flux and the corresponding normal-gravity simulations are presented in detail in this section. As mentioned above, they have not been previously reported and also contain novel data obtained with the UIS.

Temperature Data

Temperature profiles along the foam centerline are presented in Fig. 4a for the normal gravity downward simulation, in Fig. 4b for the microgravity test, and in Fig. 4c for the normal gravity upward simulation. Comparison between the temperature profiles in microgravity and in normal-gravity downward smolder shows significant differences. The temperature profiles for the microgravity tests show an almost constant peak-temperature that follows the initial descent in the peak temperatures as the reaction propagates away from the igniter. In normal gravity the initial descent is followed by a significant increase in temperatures that leads to temperatures characteristic of char oxidation towards the end of the sample. In microgravity, only a minor temperature increase is observed at the end of the sample. Upward simulation experiments lead to extinction (Fig. 4c) once the reaction progresses beyond the area where it is influenced by the igniter. In upward opposed-propagation, the smolder front does not self-propagate, most likely as a result of the opposition of the forced flow and the buoyant flow (Walther et al. 2000).

Radial temperature measurements in microgravity testing, not presented here, indicate that the reaction front is nearly planar throughout the duration of the tests. This is due in part to the

uniform forced air flow velocity profile, due to the presence of diffusers at the inlet and outlet of the sample holder. In normal gravity, buoyancy enhances the air flow velocity at the center of the sample, leading to a more conical smolder propagation front.

The temperature profiles from the middle thermocouples, which are not influenced by the ignition period or by end effects, are used to calculate an average smolder velocity. Within this region the average smolder velocity in microgravity is approximately 30% lower than the corresponding normal gravity downward smolder velocity (0.19 mm/s vs. 0.25 mm/s).

These observations provide clear evidence of the role of buoyantly induced flows on the smolder propagation rates as well as on the nature of the smolder reaction.

Ultrasound Imaging Data

The permeability histories obtained from the UIS are presented in Fig. 5 for the normal gravity and microgravity tests. They represent the first data obtained from the UIS application to microgravity smolder research. The data are used to calculate the smolder reaction velocity and the permeability, and through it the level of fuel consumption and a time history of the char reactivity. Comparison of the smolder velocities calculated from the permeability and from the temperature data shows good agreement between them. The calculated average smolder velocity is 0.19 mm/s from the temperature data and 0.184 mm/s from the permeability data. For the opposed downward normal-gravity test at 3 mm/s forced airflow velocity, the average smolder velocity is 0.245 mm/s from the temperature data, and 0.241 mm/s from the permeability data. These calculations show good agreement between the velocities obtained from both thermocouple and ultrasonic histories.

In the case of upward opposed-burning, it is also observed that after the extinction of the smolder front, the steady-state values of the char permeability continue to rise slightly over a long period of time. This is likely due to the continued oxidation of the residual char by the remaining oxidizer contained in the chamber, especially in the area close to the igniter where temperatures are higher. The continued char reaction can lead to the formation of a solidified film near the transducer pairs, which can impede the transmission of the ultrasonic signal. The permeability history of the downward opposed normal-gravity test also shows a substantial jump in the permeability at the location of the last transducer pair at ~1500 s, corresponding to a similar jump in temperature at the final thermocouple. This is the result of the buoyantly driven air mass flux added to the reaction from the chamber air.

Smolder Velocity

The only available data in microgravity opposed-smolder propagation are those from the present tests (STS-105) and the two tests previously conducted in Space Shuttle missions STS-69 and 77 (Walther et al. 1999). The measured average propagation-velocities for the oxygen mass fluxes for these three experiments, (0.28, 0.56 and 0.84 g-O_2/m^2s), are presented in Table 1, together with the corresponding values from normal gravity simulations. It is seen that both in microgravity and normal gravity the smolder propagation velocity increases as the airflow velocity is increased, although the rate of increase is somewhat different. The smolder velocity for the forced 0.84 g-O_2/m^2s microgravity experiment seems to have a smaller value than expected according to the normal gravity tests. Since this last test was conducted with a different sheath material and ignition protocol than the previous ones, normal-gravity simulations were conducted to determine if the changes in sheath and ignition protocol affected the smolder velocity, but no significant difference in smolder velocity was observed. Another possible explanation is the ageing of the polyurethane foam used (Dement'ev et al. 1999). Unfortunately,

at this point it is not feasible to repeat the experiment in microgravity, thus it cannot be concluded if the forced 0.84 g-O_2/m^2s microgravity data are accurate, or are affected by a higher experimental random inaccuracy.

Comparison of the microgravity and normal gravity data shows that, at least in the range of airflows tested, the microgravity smolder velocity lies between the corresponding upward and downward normal-gravity smolder. This is to be expected since at these flow conditions, smolder propagation is strongly dependent on the flux of oxygen to the smolder reaction (Ohlemiller 1985). In normal-gravity downward propagation, the buoyant flow adds to the forced flow; while in the upward case, the buoyant flow opposes (and partially cancels) the forced flow.

III.2 Dependence of the Smolder Velocity on Ambient Pressure

As explained above, because the MSC combustion chamber is sealed, in the microgravity forced-flow tests the chamber ambient pressure increases as the experiment progresses due to the addition of air and the increase in temperature of the chamber gases. This experimental fact can be used to study the effect of buoyancy on the smolder propagation velocity by calculating the smolder velocity locally, rather than averaging it as done to obtain the results of Table 1, and correlating it with the average pressure during the corresponding time interval. In addition experiments were also conducted maintaining the chamber pressure constant to study the effect of the ambient pressure on forced downward opposed-smolder. In these tests, the smolder velocity reported is that measured in the center region of the sample away from end effects (Torero et al. 1993). The results are presented in Fig. 6 for opposed smolder in normal- and microgravity. It is seen that the smolder propagation velocity increases as the ambient pressure increases in normal gravity, but only slightly increases in microgravity, indicating that the effect is probably related more to buoyancy effects than chemical kinetics. The trend is in agreement with the results of Newhall et al. (1989) for the smolder of cellulose, further verifying the buoyant character of the pressure effect.

From the results of Fig. 6 it is observed that under similar ignition conditions and sample size, there exists a minimum ambient pressure at which a self-sustaining smolder reaction is achieved. In the microgravity tests, this minimum pressure is approximately 1 atm, although it is difficult to quantify the velocity at this minimum pressure because initially smolder occurs under the influence of the igniter and at a reduced oxidizer mass flux. In the forced-flow normal-gravity tests this minimum pressure depends on the forced oxygen-mass flux, decreasing with it. At a forced oxygen-mass flux of 0.28 g/m^2s, the minimum pressure is 1.96 atm; at a forced oxygen-mass flux of 0.56 g/m^2s the minimum pressure is 1.45 atm; and finally at a forced oxygen-mass flux of 0.84 g/m^2s the minimum pressure is 1.26 atm. Since smolder is strongly dependent on the oxidizer flux at the reaction front, and the pressure effects seem buoyancy related, these results point to a minimum mass flux of oxidizer for smolder to self propagate.

Fig. 7 shows the peak reaction-temperatures as a function of axial position in the sample for the 0.56 g-O_2/m^2s forced oxygen-mass flux experiment in microgravity and for the same forced oxygen-mass flux in normal gravity at a range of pressures. Close to the igniter, the reaction temperatures in both normal- and microgravity are highest due to strong influence from the igniter. In the microgravity case, the reaction temperature is observed to rise only slightly with position in the sample. This is likely due to the increasing pressure in the microgravity experiment, leading to a slight effect on the kinetics of the smolder reaction and hence on the reaction temperature. In the normal-gravity case, for pressures of 1.36 atm and below the reaction temperature is seen to uniformly decrease through the length of the sample. This is characteristic of extinction of the reaction for cases where no propagation was seen. In the range of pressure

from 1.36 atm to 3.06 atm, the reaction temperature away from the igniter (at an axial position of 20 mm and greater) is seen to increase with axial position. The rate of increase is more important than for the microgravity experiment. This is strong evidence of an increasing contribution from the buoyant mass-flux consistent with an increase in the char permeability. At pressures of 3.06 atm and above, a sharp transition is seen in the reaction, characterized by significantly higher reaction temperatures.

IV. ANALYSIS OF THE RESULTS

The above results can be explained with a simplified analysis of the smolder process as that developed in Torero et al. (1993). Smolder propagates in a creeping fashion by the smolder reaction heating the virgin fuel ahead of it, and eventually inducing its exothermic reaction with the incoming oxidizer. Smolder often occurs under oxygen-limited conditions (Ohlemiller 1985), and consequently the rate of heat release from the smolder reaction is directly proportional to the oxidizer mass flux. The heat released by the smolder reaction is in turn partially transferred ahead of the reaction and partially lost to the surrounding environment. Under these conditions, the smolder propagation is determined by a balance between the heat released by the reaction, the energy required to heat the virgin foam and incoming air to the smolder temperature and the heat losses to the environment (Dosanjh et al. 1987). The application of such an energy balance provides the following expression for the opposed smolder propagation-velocity:

$$u_{sml} = \frac{\dot{m}''_{O_2} Q_{sml} - \dot{m}''_g c_{p,g}\left(T_S - T_a\right) - \dot{Q}''_{loss} \left/ A_L A_c \right. + \dot{Q}'''_{ig}}{\rho_s c_{p,s}\left(1-\phi\right)\left(T_S - T_a\right)} \qquad (1)$$

The terminology is given in the nomenclature section.

The heat released from the igniter is negligible when studying self-sustained smolder propagation because it occurs away from the igniter influence. For the present range of velocities, the energy required to heat the incoming air flow to the smolder temperature is small in comparison with the other energy terms. Consequently, in the above expression the two major parameters determining the smolder velocity are the heat released by the reaction and the heat losses to the external environment. Thus, in order to apply Eq. (1) to calculate the smolder velocity, it is necessary to determine the effect on the oxidizer mass flux and on the external heat losses of the problem parameters (forced air flow, buoyancy induced flow and pressure).

Oxidizer Mass Flux

The total oxidizer mass flux to the reaction zone is a combination of the forced flow, the buoyancy-induced flow, and the diffusive transport.

The forced oxidizer mass flux is given by:

$$\dot{m}''_{O_2,for} = \phi \rho_g u_{for} y_{O_2} \qquad (2)$$

For the present experiments, the forced mass flux is controlled through a critical nozzle (in microgravity) or a mass flow controller (in normal gravity), and is therefore constant and known for a given test.

In the presence of gravity, a buoyant flow is induced through the porous material. The driving force of this flow is the difference in densities between the hot gases leaving the reaction zone and the surrounding cold fresh air. There are two main mechanisms that can induce this flow (Torero 1993); one is a natural draft along the whole sample length (chimney like) and the other is a boundary layer flow generated at the duct walls by the temperature difference of the gas near the wall and the porous char. Based on experimental observations and previous analysis (Torero 1993), the authors think that both mechanisms are present in these experiments. Therefore the exact calculation of the buoyant flow could be quite complex. The accuracy by which the flow fields within the porous media can be calculated depend on many parameters that cannot be estimated appropriately for the present experiments, thus these computations reside outside the scope of this work. Nevertheless, since both the natural draft and the boundary-layer flow share the same driving force, the buoyant flow can be approximately quantified using dimensional analysis. For mixed convection in porous media through a vertical duct, the governing non-dimensional parameter is the ratio of the Grashof number to the Reynolds number Gr_K/Re_K, when the Darcy parameter K_{CH}/D^2 has a low value (Lai et al. 1990), which is the case of the present experiments (~10^{-7}). Consequently, it can be inferred that the ratio of the buoyant velocity to the forced velocity $\frac{u_{buo}}{u_{for}}$ is proportional to this non-dimensional parameter, i.e., $\frac{u_{buo}}{u_{for}} = C_0 \frac{Gr_K}{Re_K}$, where the constant of proportionality, C_0, will depend on the experimental configuration and the particular mechanism that induces the buoyant flow. For flow in porous media, the Grashof and Reynolds numbers are usually defined as follows:

$$Gr_K = \frac{\sqrt{K_{CH}^3}\, g \rho_g^2 \beta (T_S - T_a)}{\mu^2} \tag{3}$$

$$Re_K = \frac{\rho_g u_{for} \sqrt{K_{CH}}}{\mu} \tag{4}$$

Then, the non-dimensional gas velocity is given by the expression:

$$\frac{u_{buo}}{u_{for}} = C_0 \frac{K_{CH} g \rho_g \beta (T_S - T_a)}{u_{for} \mu} \tag{5}$$

from which, the buoyant oxidizer mass flux is calculated as:

$$\dot{m}''_{O_2,buo} = \phi \rho_g u_{bou} y_{O_2} = C_0 \frac{K_{CH} g \rho_a{}^2 \beta \phi y_{O_2} (T_S - T_a)}{\mu} P^2 \tag{6}$$

For mixed convection, if the parameter Gr_K/Re_K is in the order of unity (in our experiments it ranges from 1 to 5), both forced and buoyant flows are important and the total flux is better express as a quadratic combination (Incropera and DeWitt 1996):

$$\dot{m}''_{O_2,t} = \sqrt{(\dot{m}''_{O_2,for})^2 \pm (\dot{m}''_{O_2,bou})^2} \tag{7}$$

The buoyant flow assists or opposes the forced flow depending on the sample orientation (downward or upward). The normal-gravity experiments in Fig. 6 were in the downward opposed configuration, and therefore the buoyant and forced fluxes add.

The third source of mass flux is that generated by diffusive transport, which is given by:

$$\dot{m}''_{O_2,dif} = \rho_g D_{bd} \frac{\partial y_{O_2}}{\partial x} \tag{8}$$

For a diffusion coefficient of 10^{-5} m^2/s and air as oxidizer, the diffusive mass flux of oxygen can be estimated as 0.02 g/m^2s. In normal gravity this value is significantly smaller than the mass flux induced by buoyancy, and therefore the diffusive flux is only important in microgravity for low forced fluxes.

Equations (2) to (8) are used to calculate the total oxidizer-mass flux to the reaction zone. Once the total oxidizer-mass flux is calculated, the experimental results in Fig. 6 can be plotted in the form of smolder velocity vs. total oxidizer-mass, as shown in Fig. 8. The properties used to calculate the buoyant term are presented in Table 2. Smolder temperatures are obtained from thermocouple measurements, and the permeability of the char is obtained from the UIS. Theoretically, it is predicted that smolder propagation velocity depends linearly on the oxidizer-mass flux to the smolder front (Dosanjh et al. 1987). Linear optimization to the experimental data thus provides the value of constant C_0 (Table 2).

It can be seen in Fig. 8, that for a given mass flux, the microgravity smolder velocity is larger than in normal gravity. In order to achieve a smolder velocity of 0.10 mm/s with forced flow, the microgravity total oxidizer-mass flux is 0.30 g/m^2s, while the normal gravity forced flow test total oxidizer-mass flux is calculated to be around 0.60 g/m^2s. Similarly, the smolder velocity in microgravity at an oxidizer mass flux of 0.58 g/m^2s is the same as that of a normal-gravity forced-flow with an oxidizer-mass flux around 0.85 g/m^2s. These observations suggest that the presence of buoyant heat losses in normal gravity hinders the smolder reaction and that a significantly higher oxidizer-mass flux is required to obtain the same smolder propagation velocity as in microgravity. These results justify a more detailed analysis of the term $\dot{Q}''_{loss}$ in Eq. (1), as shown in the next subsection.

For the present test conditions and sample size, the experimental results of Fig. 8 also indicate that there exists a minimum critical oxidizer-mass flux to achieve a self-sustaining smolder propagation, and that this critical flux is significantly smaller in microgravity than in normal gravity, (0.3 vs. ~0.6 $g\text{-}O_2/m^2s$). This also appears to be due to the difference in heat losses between the two environmental conditions. These results have obvious important implications from the point of view of fire safety in spacecraft.

Finally, Fig. 8 shows that the points corresponding to pressures beyond 3.06 atm (labeled "transition regime") still seem to follow a linear behavior with the total oxidizer-mass flux but the slope is different. Since the slope is given by the combination of the different buoyancy driven contributions and the reactions pathways, this change in slope indicates that the change in regime is induced either by a shift in the specific mode of buoyantly driven flow controlling propagation or by a change in the foam thermal decomposition (i.e. secondary char oxidation).

Radial Heat Losses

The accurate calculation of the radial heat losses from the smolder reaction to the outside environment is a complex problem and requires numerically solving the complete heat transfer problem coupled with fluid flow. However, a simplified steady state analysis can be used to approximately calculate the heat losses if the characteristic time for smolder propagation is much greater than the characteristic time for radial thermal diffusion. The characteristic time for smolder propagation is approximately given by the ratio of the smolder reaction length to the smolder velocity. The smolder-reaction length corresponds to the region where the foam temperature rises from ambient to the smolder temperature (approximately 40 mm in these experiments). The smolder velocity is of the order of 0.1 mm/s for these experiments. Thus, the characteristic time for smolder propagation is for these experiments on the order of 400 s. Since convection is the dominant mode of radial heat transfer through the foam (as will be proven later); with a calculated heat transfer coefficient of 6 W/m^2s, an estimated thermal layer near the sample holder wall of 10 mm (from the pictures that show an unburnt region of approximately this width) and the foam thermal properties shown in Table 2, the characteristic time for thermal diffusion is 14 s. Thus the ratio of smolder propagation characteristic time to the thermal wave characteristic time is one order of magnitude, which justifies the validity of a steady state analysis of the heat losses from the smolder reaction to the surrounding environment.

Under the steady state assumption, the radial transfer of heat from the smolder reaction to the environment can be calculated by equating the heat fluxes through the foam, the sample holder wall and the outside environment. For forced flow, convection is the dominant mode of heat transfer through the foam. Across the sample holder wall, conduction is the only heat-transfer mechanism. Whereas heat transfer to the surrounding air occurs primarily by conduction in microgravity, and by natural convection in normal gravity. Thus the radial heat losses can be approximately calculated from the expressions:

$$\dot{Q}''_{loss,mg} = \frac{T_{m,mg} - T_a}{\frac{1}{h_i} + \frac{e}{k_w} + \frac{L_0}{k_0}} \tag{9}$$

in microgravity, and by:

$$\dot{Q}''_{loss,1g} = \frac{T_{m,1g} - T_a}{\frac{1}{h_i} + \frac{e}{k_w} + \frac{1}{h_0}} \tag{10}$$

in normal gravity.

Where $T_m = (T_S + T_a)/2$ (11)

For forced convection in a porous media it is found that for non-fully developed flow, the Nusselt number is given by the following experimental correlation (White 1988, Nield and Bejan 1992):

$$\mathrm{Nu_D} = \frac{h_i D}{k_{eff}} = 5.856 + \frac{\dfrac{0.1069}{\lambda}}{\left(1 + \dfrac{0.04}{\lambda^{2/3}}\right)} \tag{12}$$

where $\lambda = \dfrac{\delta}{D\,Re\,Pr}$. The sample holder wall is made of Vespel, which has a thermal conductivity of 0.56 W/mK, and its thickness is 4 mm. In microgravity, heat transfer across the quiescent air surrounding the sample holder is primarily by conduction. Experimentally, it is determined that the chamber temperature is maintained constant at ambient temperature T_a. In normal gravity, heat transfer through the air surrounding the sample holder is primarily by natural convection and the corresponding Nusselt number is given by (Incropera and DeWitt 1996):

$$\mathrm{Nu}_\delta = \frac{h_0 \delta}{k_0} = \left(0.825 + \frac{0.387 \mathrm{Ra}_\delta^{1/6}}{\left(1 + \left(0.492/\mathrm{Pr}\right)^{9/16}\right)^{8/27}} \right)^2 \tag{13}$$

where the Rayleigh number is defined as $\mathrm{Ra}_\delta = \dfrac{g\beta\Delta T \rho_a \delta^3}{\mu\alpha} P^2$.

The radial heat losses predicted by applying Eq. (9) and (10) are calculated using the properties in Table 2, and the results shown in Fig. 9 as a function of the total gas-mass flux. Note that normal gravity heat-loss depends also on pressure, a variable that is not shown explicitly in Fig. 9, and which causes the small scattering observed in the results. The analysis predicts that the radial heat losses to the environment are up to seven times larger in normal gravity than in microgravity. This confirms the above statement that heat losses are a primary reason for the differences observed between normal gravity and microgravity data.

Correlation of the smolder velocity

Once the oxidizer-mass flux and heat losses are determined, the energy balance of Eq. (1) can be used to calculate theoretically the smolder velocity away from the igniter. The predicted smolder propagation velocities as a function of the oxidizer-mass flux are shown in Fig. 8 for both normal gravity and microgravity, together with the experimental data. The values for the parameters used in the calculation are shown in Table 2. The heat of combustion for smoldering, Q_{sml}, has not been yet well determined (Ohlemiller 1985). In this study, the heat of smoldering is selected such that the correlation of the microgravity experimental data with Eq. (1) is optimized. The resulting value of 5880 kJ/kg-O_2 is larger than the values reported in previous studies: 3900 kJ/kg-O_2 (Torero et al. 1993) and 4550 kJ/kg-O_2 (Walther et al. 1999). The authors feel that the present value is more accurate since the previous studies optimized the correlation of the experimental data without explicitly considering the heat losses, thus the values they presented incorporate the heat losses effect into the heat of combustion. The predicted results of Fig. 8 show that Eq. (1) captures most of the dependence of the smolder velocity on the experimental parameters, even though the analysis is based on a simplified energy balance and approximate calculations of the oxidizer-mass flux and the heat losses.

The predicted normal-gravity smolder velocity is lower than that in microgravity for the same oxidizer-mass flux, as observed experimentally. Based on Equation (1), the intercept of the line to the data is supposed to provide the critical total mass flux of oxidizer for smolder propagation. The analysis, however, cannot predict the minimum critical flux for smolder because under these conditions, the smolder reaction is close to extinction and becomes strongly affected by chemical kinetics, truncating the linear dependency. The analysis is thermal and does not consider chemical kinetic aspects of the process. However, from the analysis it can be inferred that heat losses partially explain the lower critical oxidizer mass flux for propagation in microgravity.

Eq. (1) can also be used to predict the behavior of the smolder velocity with pressure, as shown in Fig 6 (by the lines) that plots predicted smolder velocity vs. pressure. At low pressures, the plateau in the predicted smolder velocity is caused by the smolder propagation being dominated by the forced flow. At higher pressures, the smolder propagation is dominated by the buoyant flow and the different forced-flow tests converge to the same smolder velocity. Note that as pressure increases, the variation in total oxidizer-mass flux between different forced flows decreases. The reasonable agreement between theory and experiments indicates that the effects of pressure on buoyant transport dominate over the effects on chemical kinetics. In addition, analysis of the microgravity data shows that the effects of pressure on the smolder velocity are on the order of $P^{1/3}$, which must be due to chemical kinetics effects.

V. CONCLUDING REMARKS

A comparison of the tests conducted in normal gravity and microgravity indicates that for a given sample size there is a critical oxidizer-mass flux to attain a self-propagating smolder reaction, and that this critical mass flux is significantly smaller in microgravity than in normal gravity. This finding has important implications from the point of view of fire safety in a space-based environment since smolder can be initiated at lower oxygen concentrations or mass flows than in normal gravity.

The primary effect of pressure is on buoyancy-induced transport. Results and analysis indicate that buoyancy-induced heat losses greatly affect the smolder propagation, since their removal in microgravity tests allows for self-sustained smolder propagation at oxidizer-mass fluxes below the critical minimum oxidizer-mass flux observed in normal-gravity tests. Since buoyant heat losses are the primary reason for these results, then quantitative differences will be observed for the critical mass fluxes as a function of the sample size, decreasing as the sample size increases. Quantitative differences will also strongly depend on any additional external insulating or heat-conducting conditions. Analytical modeling of diffusion transport indicates that the diffusive mass flux accounts for only a small fraction of the total oxidizer-mass flux. This is strongly evidenced by tests conducted in a quiescent environment in microgravity, for which no self-sustained smolder propagation was observed. The results also indicate that smolder chemical kinetics display only a weak pressure dependence.

The analysis also suggests that narrow samples are subjected to greater heat loss relative to the heat generated from the reaction. This had been observed by tests conducted on 50 mm diameter, 80 mm length cylindrical samples of polyurethane foam aboard the NASA USML-1 mission (Stocker et al. 1996). In these tests, no self-sustained propagation of a smolder reaction was observed in samples of this size.

ACKNOWLEDGEMENTS

This work was supported by the National Aeronautics and Space Administration, under NASA grant NAG3-2026. The authors would like to acknowledge the work and support during the development of this work of the NASA Glenn engineering team. Also, our thanks go to Mr. R. Medina, Mr. T. Lo, Ms. S. Fereres, Mr. O. Putzeys, Mr. M. Heath, Mr. R. Titus and Mr. Y.F. Lo, who assisted running experiments.

REFERENCES

Babrauskas, V., (1996) "The Results of a Major Upholstered Furniture Fire Study", *National Fire Protection Association Journal* 90, pp. 84-88.

Burrough, B. (2000) *Dragonfly: NASA And The Crisis Aboard Mir*. HarperCollins, New York.

Damant, G.H. (1994), "Recent United States Developments in Tests and Materials for the Flammability of Furnishings", *Journal of The Textile Institute*, Vol. 85 (4), pp. 505-525.

Dement'ev, M.A, Demina, A.I. and Nevskii, L.V. (1999), "Ageing and Salvaging of Flexible Polyurethane Foam under Atmospheric Conditions", *International Polymer Science and Technology*, Vol. 26, No. 4, pp. 89-92.

Dosanjh, S.S., Pagni P.J. and Fernandez-Pello, A.C. (1987) "Forced Cocurrent Smoldering Combustion", *Combustion and Flame*, Vol. 68, pp.131-142.

Friedman, R. (1993) "Risk and Issues in Fire Safety on The Space Station", NASA Technical Memorandum 106403.

Hall, J.R. (2003) "The Smoking-Material Fire Problem" Report prepared for the National Fire Protection Association, May 2003. Available at http://www.nfpa.org.

Incropera, F.P. and DeWitt, D.P. (1996) *Introduction to Heat Transfer*. Third edition, John Wiley & Sons (Ed.).

Lai, F.C., Kulacki, F.A. and Prasad, V. (1991), "Mixed Convection in Saturated Porous Media", *Convective Heat and Mass Transfer in Porous Media*. NATO ASI Series, Kluwer Academic (Ed.). pp. 225-288.

Newhall, J., Pagni, P.J., Fernandez-Pello, A.C. (1989) "Experimental Observations of the Effect of Buoyancy on Co-Current Smoldering", *Journal of Fire and Materials*, Vol. 14, pp. 145.

Nield, D.A. and Bejan, A. (1992) *Convection in Porous Media*, Springer-Verlag (Ed.) New York.

Ohlemiller, T.J. (1985), Modeling of Smoldering Combustion Propagation, *Progress in Energy and Combustion Science*, Vol. 11pp. 277-310.

Ross, H.D. (1997) "Burning To Go: Combustion On Orbit and Mars". Invited talked, *Meeting of the Eastern States Section of The Combustion Institute*, Hartford Connecticut, Oct. 1997.

Stocker, D.P., Olson S.L., Urban, D.L, Torero, J.L., Walther, D.C, Fernandez-Pello, A.C. (1996) "Small Scale Smoldering Combustion Experiments in Microgravity", *Twenty-Sixth Symposium (International) on Combustion*, The Combustion Institute, pp. 1361-1368.

Torero, J.L, (1993) "Buoyant Effects on Smoldering of Polyurethane Foam", Ph.D. Thesis, Department of Mechanical Engineering. *University of California*, Berkeley.

Torero, J.L., Fernandez-Pello, A.C. and. Kitano, M (1993) "Opposed Forced Flow Smoldering of Polyurethane Foam" *Combustion Science and Technology*, Vol. 91, No. 1-3, pp. 95-117.

Tse, S.D., Anthenien, R.A., Fernandez-Pello, A.C. and Miyasaka, K. (1999) “An Application of Ultrasound Tomographic Imaging to Study Smoldering Combustion” *Combustion and Flame*, Vol. 116, No. 12, pp.120-135.

Walther, D.C., Fernandez-Pello, A.C. and Urban, D.L. (1999) “Space Shuttle Based Microgravity Smoldering Combustion Experiments”, *Combustion and Flame*, Vol. 116, No. 3, pp. 398-414.

Walther, D.C., Anthenien, R.A. and Fernandez-Pello, A.C. (2000) “Smolder ignition of polyurethane foam: effect of oxygen concentration”, *Fire Safety Journal*, Vol. 34, No. 4, pp. 343-359.

White, F.M. (1988), *Heat and Mass Transfer*, Addison-Wesley (Ed.).

NOMENCLATURE

Symbol	Definition
A_l/A_c	Lateral to cross sectional area ratio for the smolder front volume
C_0	non-dimensional constant
$c_{p,s}$	Specific heat of the solid
$c_{p,g}$	Specific heat of the gas
D	Diameter of the sample holder
D_{bd}	Binary diffusion coefficient
e	Thickness of the sample holder wall
g	Gravity acceleration
h_i	Convection heat transfer coefficient in the porous media
h_0	Natural convection heat transfer coefficient
k_0	Thermal conductivity of the gas in the chamber
k_{eff}	Thermal conductivity of the porous foam
k_w	Thermal conductivity of the sample holder wall
K	Permeability
L_0	Distance from the sample holder to the chamber wall
$\dot{m}''_{O_2}$	Oxygen-mass flux to the smolder front
$\dot{m}''_g$	Gas-mass flux to the smolder front
Nu	Nusselt number
Pr	Prandtl number
P	Pressure
$\dot{Q}''_{ig}$	Igniter heat flux
$\dot{Q}''_{loss}$	Heat loss flux
Q_{sml}	Heat of combustion for smoldering
Ra	Rayleigh number
Gr_K	Grashof number based on permeability
Re	Reynolds number
Re_K	Reynolds number based on permeability
T_a	Ambient temperature
T_S	Characteristic temperature of smolder
T_m	Mean temperature
u	Gas velocity
u_{sml}	Smolder front propagation velocity
x	Axial distance from top edge of sample
y_{O2}	Mass fraction of oxygen

Greek symbols

b	Volumetric thermal expansion coefficient
d	Thickness of the smolder front
f	Porosity of the foam
λ	Graetz number
ρ_s	Density of the solid
ρ_g	Density of the gas
μ	Gas dynamic viscosity

Subscripts

1g	Normal gravity conditions
μg	Microgravity conditions
a	Ambient conditions
buo	Buoyant
C	Cold gas mixture
CH	Char
dif	Diffusion
for	Forced
g	Gas
H	Hot gas mixture
s	Solid
sml	smolder
t	total

Tables Captions

Table 1 Smolder velocity and temperature for varying oxidizer mass fluxes in normal and microgravity.

Table 2. Properties and parameters used in the calculations.

Figures Captions

Figure 1. Schematic of the MSC chamber and hardware.

Figure 2. Photographs of the MSC sample holder, chamber and apparatus.

Figure 3. Testing configurations for opposed forced flow.

Figure 4. Temperature histories of the; a) normal-gravity downward simulation; b) STS-105 microgravity and; c) normal-gravity upward simulation experiments.

Figure 5. Permeability histories of the; a) normal-gravity downward simulation; b) STS-105 microgravity and; c) normal-gravity upward simulation experiments.

Figure 6. Marks; measured microgravity and normal gravity smolder velocity vs. pressure. Lines; predicted microgravity and normal gravity smolder velocity vs. pressure. In the legend, experiments are named after the corresponding forced mass flux of oxidizer in [g/m^2s].

Figure. 7. Measured smolder reaction temperatures as a function of axial position for a forced oxidizer mass flux of 0.56 g-O_2/m^2s in the microgravity case, and for a forced oxidizer mass flux of 0.56 g-O_2/m^2s for the normal-gravity cases at a range of pressures from 1 to 3.4 atm.

Figure 8. Marks; measured smolder velocity vs. total oxidizer mass flux for microgravity and normal-gravity experiments. Lines; predicted and measured smolder velocity vs. oxidizer mass flux, for microgravity and normal gravity. In the legend, normal gravity flows are name after the corresponding forced mass flux of oxidizer in [g/m^2s].

Figure 9. Predicted heat loss flux vs. gas mass flux. Microgravity and normal-gravity forced-flow experiments. Note that pressure is not explicitly shown as a variable, therefore the solid line for normal gravity represents a good fit to scattered values.

Forced Air Flow Rate [g-O_2/m^2s]	Smolder Velocity [mm/s]		Smolder Temperature [°C]	
	1g	0g	1g	0g
0.28	0.125	0.10	405	385
0.56	0.180	0.18	424	410
0.84	0.245	0.19	472	412

Table 1. Smolder velocity and temperature for varying oxidizer mass fluxes in normal- and microgravity.

Quantity	Units	Value
$T_{s,1g}$	[°C]	450
$T_{s,\mu g}$	[°C]	400
T_a	[°C]	25
D	[m]	0.12
e	[m]	0.004
δ	[m]	0.04
K_{CH}	[m^2]	4.00E-09
g	[m/s^2]	9.81
μ	[Ns/m^2]	2.60E-05
ρ_0	[kg/m^3]	1.22
Q_{sml}	[kJ/kg-O_2]	5880
$c_{p,s}$	[kJ/kgK]	1.70
$c_{p,g}$	[kJ/kgK]	1.03
ρ_s	[kg/m^3]	1034
$k_{s,eff}$	[W/mK]	0.061
k_w	[W/mK]	0.56
Y_{O2}	-	0.23
β	-	2.00E-03
ϕ	-	0.975
A_L/A_C	-	1.33
C_0	-	0.38

Table 2. Properties and parameters used in the calculations.

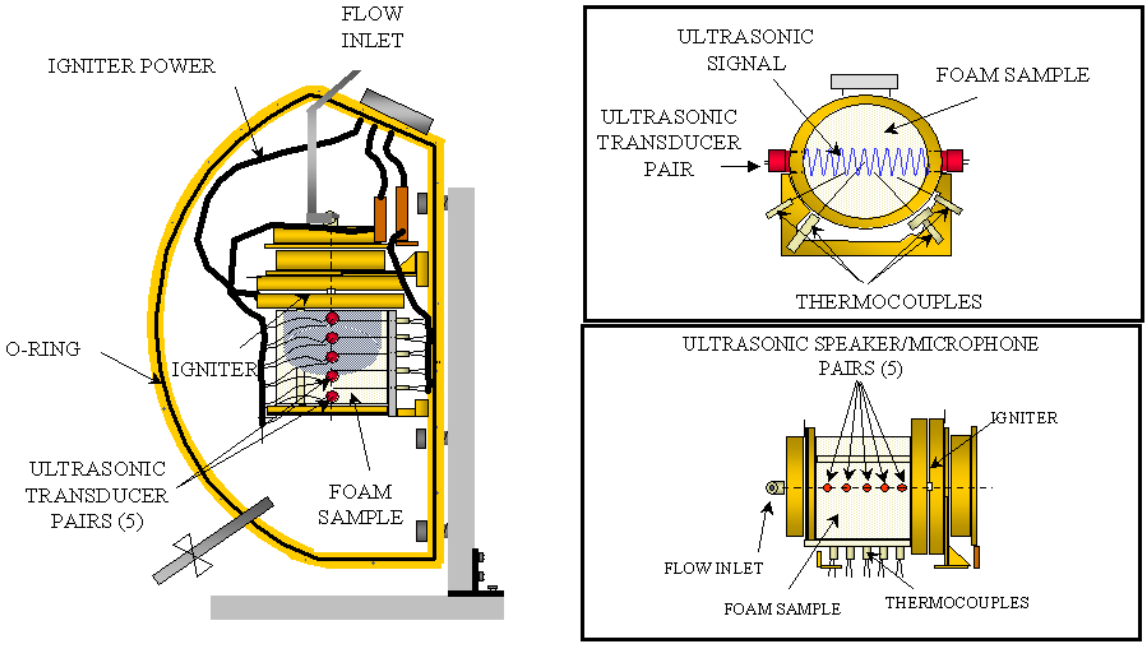

Figure 1. Schematic of the MSC chamber and hardware.

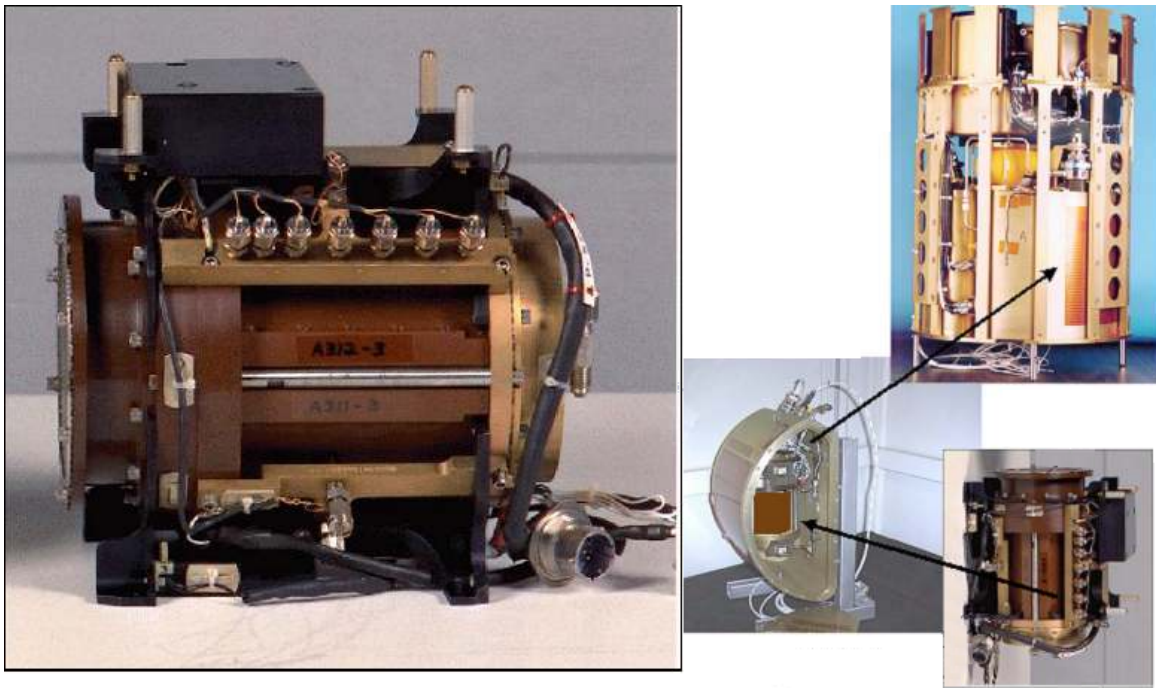

Figure 2. Photographs of the MSC sample holder, chamber and apparatus.

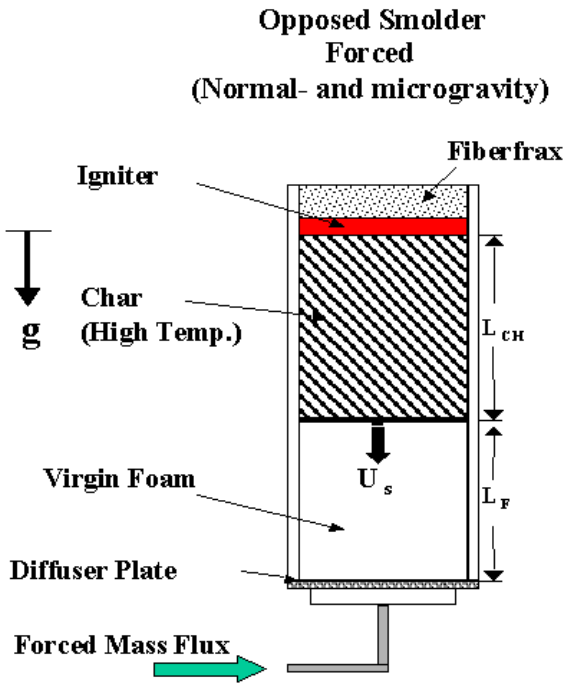

Figure 3. Testing configurations for opposed forced-flow.

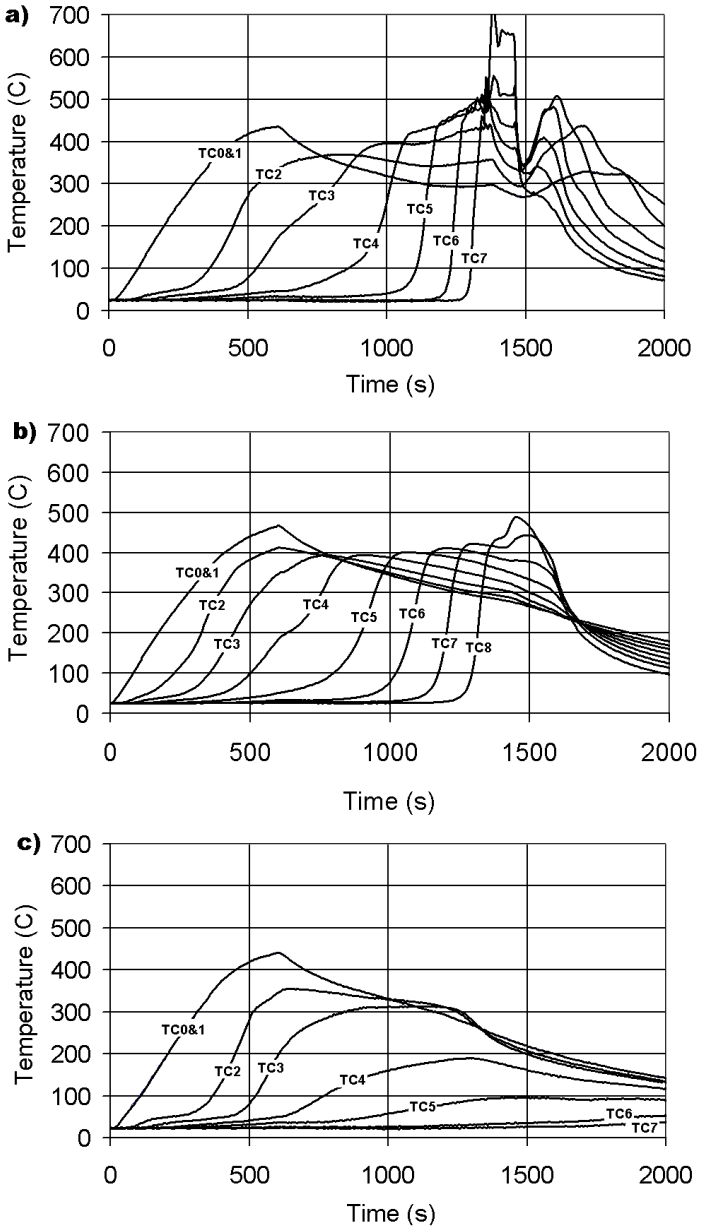

Figure 4. Temperature histories of the; a) normal-gravity downward simulation; b) STS-105 microgravity and; c) normal-gravity upward simulation experiments.

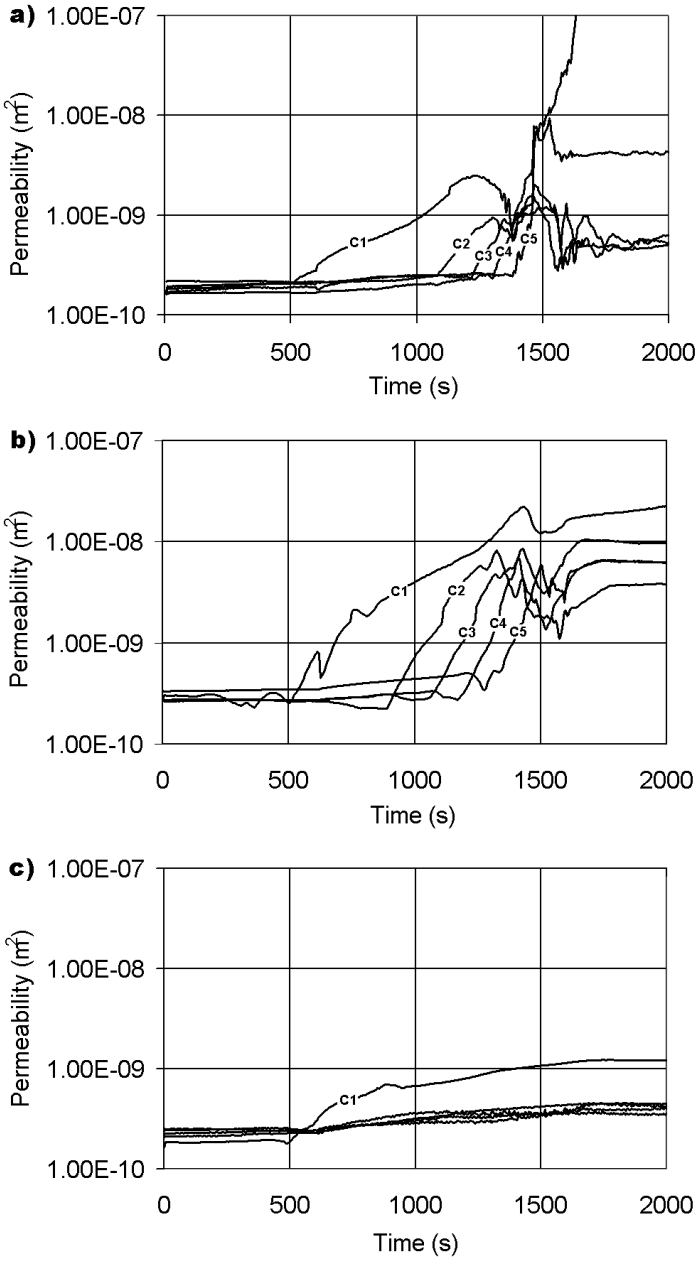

Figure 5. Permeability histories of the; a) normal-gravity downward simulation; b) STS-105 microgravity and; c) normal-gravity upward simulation experiments.

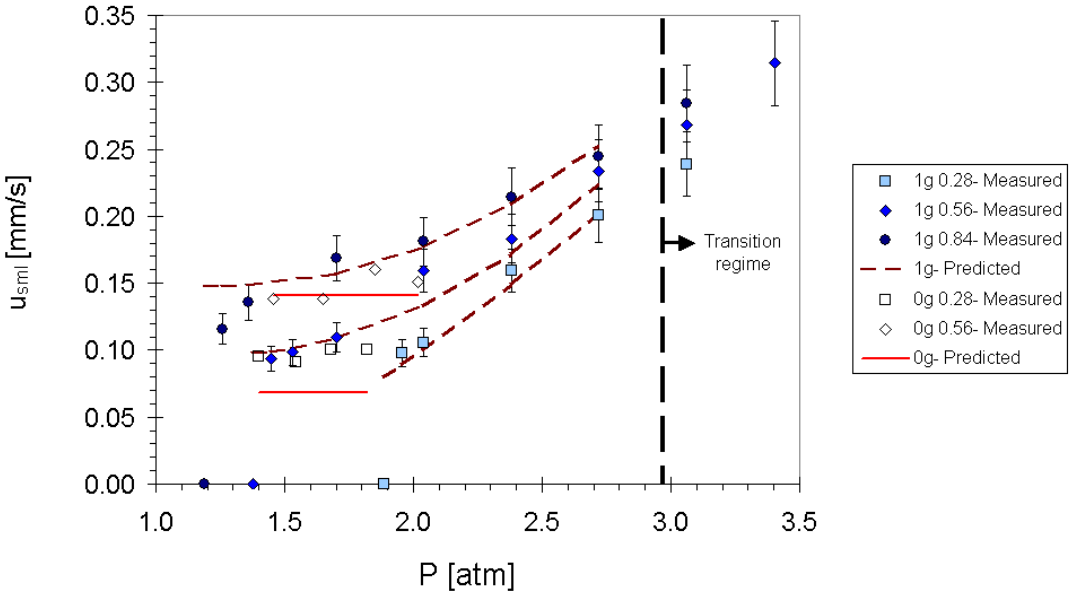

Figure 6. Marks; measured microgravity and normal gravity smolder velocity vs. pressure. Lines; predicted microgravity and normal gravity smolder velocity vs. pressure. In the legend, experiments are named after the corresponding forced mass flux of oxidizer in [g/m^{2}s].

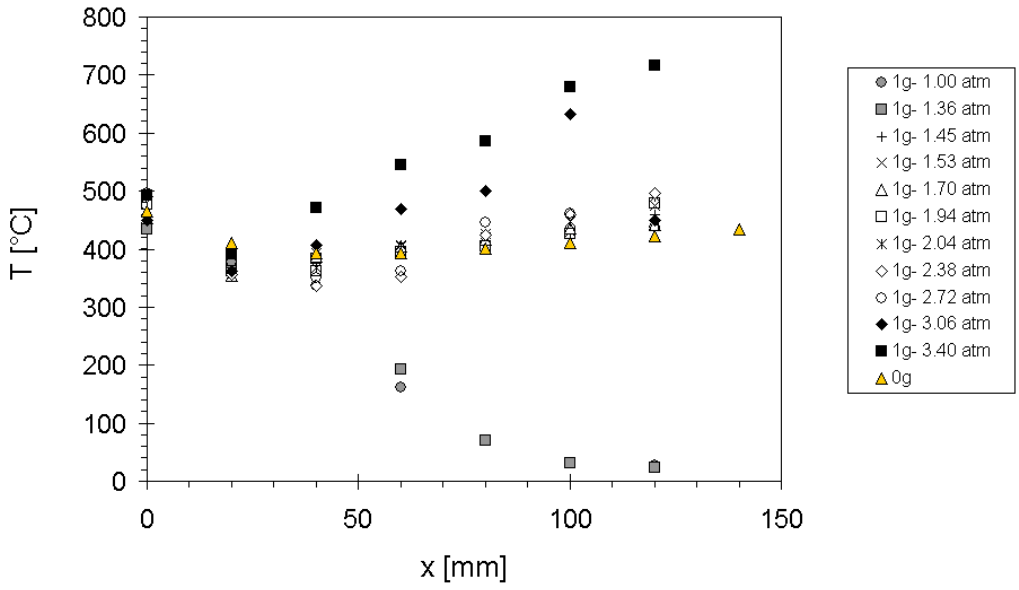

Figure. 7. Measured smolder reaction temperatures as a function of axial position for a forced oxidizer mass flux of 0.56 g-O_2/m^2s in the microgravity case, and for a forced oxidizer mass flux of 0.56 g-O_2/m^2s for the normal-gravity cases at a range of pressures from 1 to 3.4 atm.

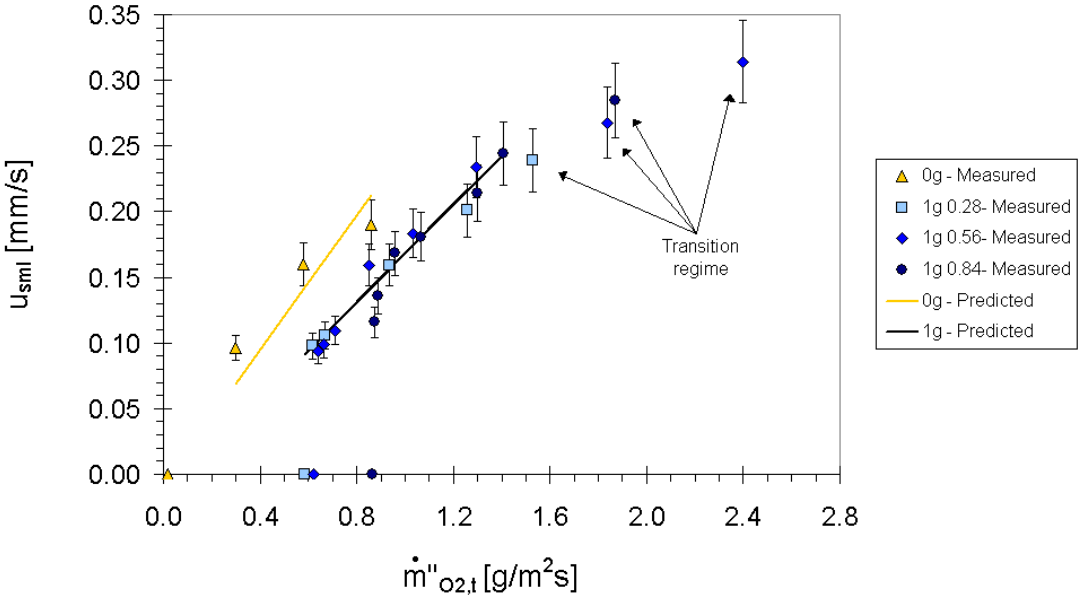

Figure 8. Marks; measured smolder velocity vs. total oxidizer mass flux for microgravity and normal-gravity experiments. Lines; predicted and measured smolder velocity vs. oxidizer mass flux, for microgravity and normal gravity. In the legend, normal gravity flows are name after the corresponding forced mass flux of oxidizer in [g/m^{2}s].

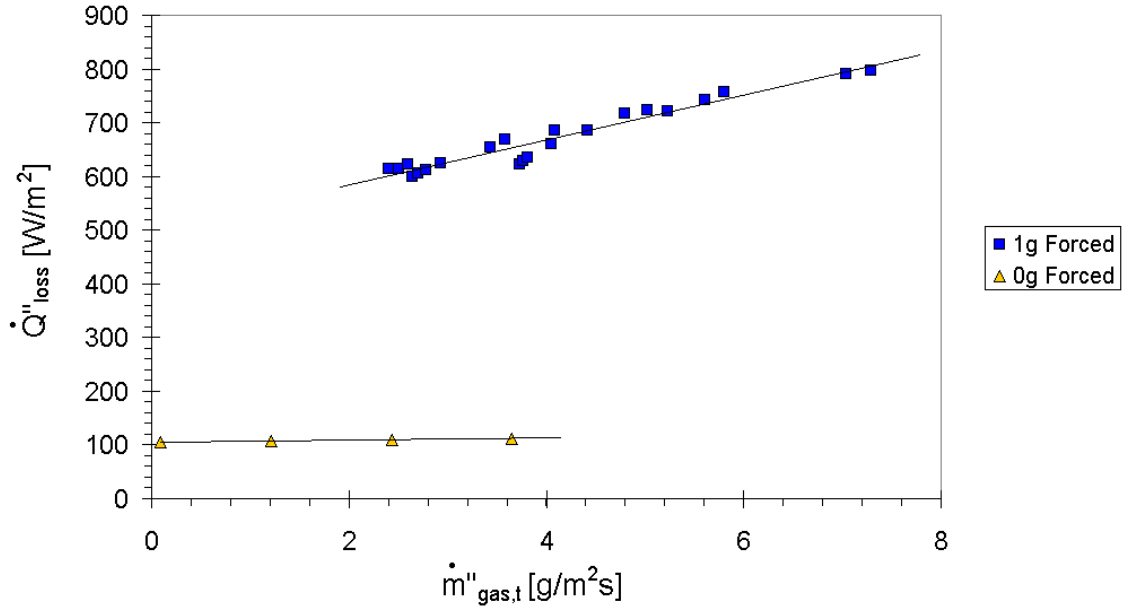

Figure 9. Predicted heat loss flux vs. gas mass flux. Microgravity and normal-gravity forced-flow experiments. Note that pressure is not explicitly shown as a variable, therefore the solid line for normal gravity represents a good fit to scattered values.